CARBON letters

Note

Carbon Letters Vol. 26, 112-116 (2018)

Preparation of fluorinated graphite with high fluorine content and high crystallinity

Min-Jung Jung, Hye-Ryeon Yu, and Young-Seak Lee*

Department of Chemical Engineering and Applied Chemistry, Chungnam National University, Daejeon 34134, Korea

Article Info

Received 15 November 2017
Accepted 9 January 2018

***Corresponding Author**
E-mail: youngslee@cnu.ac.kr

Open Access

DOI: http://dx.doi.org/10.5714/CL.2018.26.112

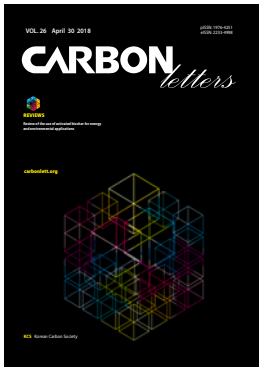

http://carbonlett.org

pISSN: 1976-4251
eISSN: 2233-4998

Fluorinated carbons are used in many applications. In particular, graphite fluoride is the most widely known material among fluorinated carbons. Because of their high chemical and thermal stability and their useful electrochemical properties, graphite fluorides have been intensively studied for use as solid lubricants with extremely low surface energies and for application as cathode material in high-energy-density lithium batteries [1-3].

Graphite fluoride $(CF)_n$ was first synthesized by Ruff and Bretschneider by the reaction of elemental fluorine with graphite at 420°C [4]. Generally, fluorine directly reacts with graphite above 350°C to give $(CF)_n$, $(C_2F)_n$, or a mixture of these, depending on the crystallinity of the original graphite and the reaction temperature [5]. Defects in the graphite structure occur due to the etching effect of fluorination [6]. In graphite fluoride, fluorine is intercalated into graphite, and its crystallinity is different from that of graphite. It is considered that graphite having high crystallinity and a high concentration of fluorine has different properties from graphite fluoride.

The graphite structure is reduced and destroyed by direct fluorination [7]. It is very difficult to maintain the graphite structure while having fluorine on the surface. Therefore, in this study, fluorinated graphite with a high fluorine content and high crystallinity was prepared by a simple and facile direct fluorination method. Most methods developed in previous research require a long reaction time (at least 12 h and 2 to 3 wk at most) or a catalyst to prepared highly fluorinated graphite [8,9]. However, the direct fluorination method used in this study has the advantage that the reaction time is relatively short and no catalyst is needed.

Graphite powder (synthesis, particle size: <20 μm, Sigma–Aldrich, USA) was treated by direct fluorination. The samples were loaded into a reactor in a nickel boat and degassed at 200°C for 2 h to remove impurities, such as water. After the degassing process, the temperature of the reactor was lowered to 25°C in a vacuum state. Fluorine gas (99.8%, Messer Griesheim GmbH, Germany) was injected at 1.0 bar, and then the temperature of the reactor was increased to 400°C for 10°C/min and maintained for 30 min. After 30 min, non-reacted gas was degassed by vacuum, and then the temperature of the reactor was quickly increased to 600°C for 20 min. After reaction, the reactor was rapidly cooled to below room temperature. For comparison, fluorination of graphite was conducted at 400°C. Another sample was annealed at 600°C in a N_2 atmosphere in a tubular furnace after fluorination at 400°C. The pristine and prepared graphite samples were labeled as RG, G-4F (fluorinated graphite at 400°C), G-4F-6V (Heat treatment at 600°C in vacuum after fluorination), and G-4F-6N (Heat treatment at 600°C in N_2 atmosphere after fluorination).

X-ray photoelectron spectra (XPS) were obtained using a MultiLab 2000 spectrometer (Thermo Electron Corporation, UK) to identify the elements present in the samples. In addition, the change in the degree of crystallization in graphite was investigated using an X-ray diffraction (XRD) apparatus (D/MAX-2200 Ultima/PC, Rigaku, Japan).

The atomic ratio of each element obtained by XPS on the surface of graphite is listed in Table 1. All samples showed distinct carbon and oxygen. Fluorine was found on the directly fluorinated graphite. After fluorination at 400°C, 20.3 at% of fluorine was introduced on graphite. The G-4F could be represented as $C_{3.7}F$. Despite being annealed at the high temperature of 600°C in vacuum, most of the fluorine remained in G-4F-6V. The G-4F-6V could be represented as $C_{3.8}F$. However, when heat treatment at 600°C was performed in a

Table 1. X-ray photoelectron spectra surface elemental analysis parameters

	Elemental content (at%)		
	C1s	O1s	F1s
RG	94.5	5.5	0.0
G-4F	75.4	4.3	20.3
G-4F-6V	75.9	4.1	20.0
G-4F-6N	92.3	5.3	2.4

nitrogen atmosphere (G-4F-6N), it was confirmed that fluorine was decomposed by thermal decomposition.

The functional groups induced on the surface of the graphite were investigated by examining the C1s and F1s XPS peaks resulting from direct fluorination. The C1s and F1s peak were deconvoluted to several pseudo-Voigt functions (sum of Gaussian and Lorentzian functions) with a peak analysis program (Unipress Co., USA). The pseudo-Voigt function is given by the following equation [10]:

$$F(E) = H\left[(1-S)\exp\left(\left(\frac{E-E_o}{FW\ HM}\right)^2 + \frac{S}{1+\left(\frac{E-E_0}{FW\ HM}\right)^2}\right)\right],$$

where, F(E) is the intensity at energy E, *H* is the peak height, E_0 is the peak center, FWHM is the full-width at half-maximum, and S is a shape function related to both the symmetry and the Gaussian-Lorentzian mixing ratio. The survey data and deconvoluted C1s and F1s peaks are shown in Figs. 1 and 2, respectively.

In the case of RG, four main peaks were observed at 284.5, 285.4, 286.2, and 287.1 eV, which correspond to graphitic sp^2 C-C, sp^3 C-C, C-O, and C=O, respectively [11]. G-4F and G-4F-6V show a new peak at 289.1 eV that can be associated with semi-covalent C–F bonds of F species [12]. In the F1s peak of G-4F and G-4F-6V, a peak is mainly present at 688.2 eV associated with semi-covalent C–F bonds [13,14]. If x is $2 \le x \le 4$ in C_xF and the C-F bond is a semi-covalent bond, the graphite fluoride is considered a first-stage structure [14]. In the case of G-4F-6N, fluorine groups at 289.1 eV (C1s) and 688.2 eV (F1s) disappeared due to the decomposition of fluorine by heat treatment at 600°C. According to the XPS results, defluorination of fluorinated graphite was completed by thermal decomposition at 600°C in a nitrogen atmosphere. Thermal decomposition of (CF)n starts at 320 to 610°C, depending on the crystallinity [15,16].

The thermal decomposition of fluorinated graphite is different for the chemical bond of C–F: covalent and semi-covalent C–F bond.

Covalent C–F bond [17,18]:

$$4CF \rightarrow C + CF_4 (or\ 8/3C + 2/3C_2F_6, or\ 5/2C + 1/2C_3F_8)$$

Semi-covalent C–F bond [20]:

$$CF_n \rightarrow C + n/2F_2$$

As seen in Figs. 1 and 2, the C–F bonds of fluorinated graphite in this experiment were mostly semi-covalent bonds. Therefore, it believed that F_2 could be generated as the decomposition gas at thermal decomposition. In a study by Sato et al. [21], the

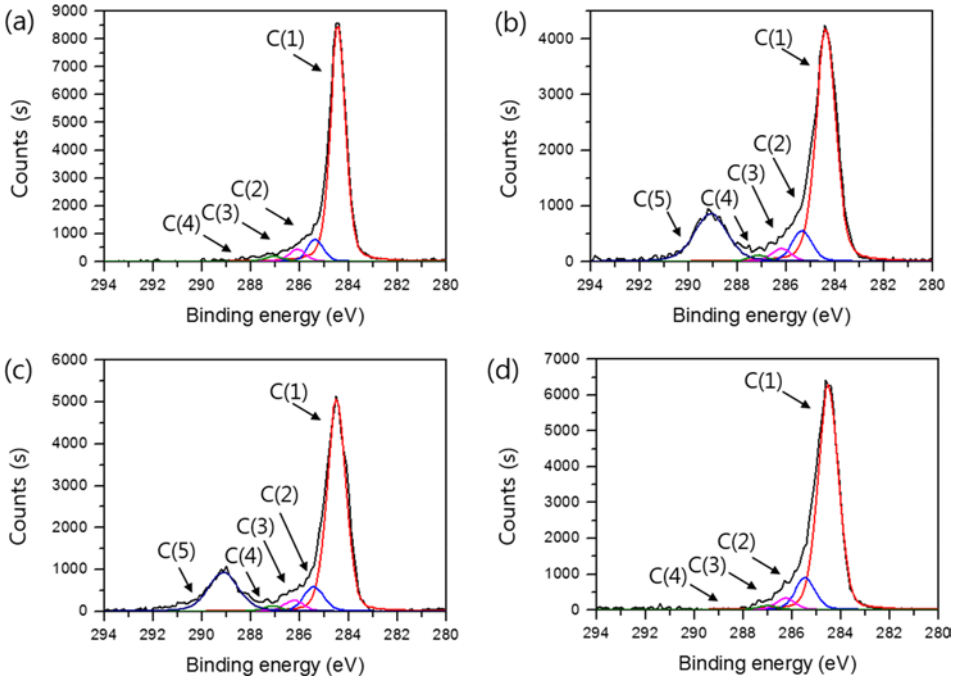

Fig. 1. Deconvolution of the core-level C1s spectra of (a) RG, (b) G-4F, (c) G-4F-6V, and (d) G-4F-6N.

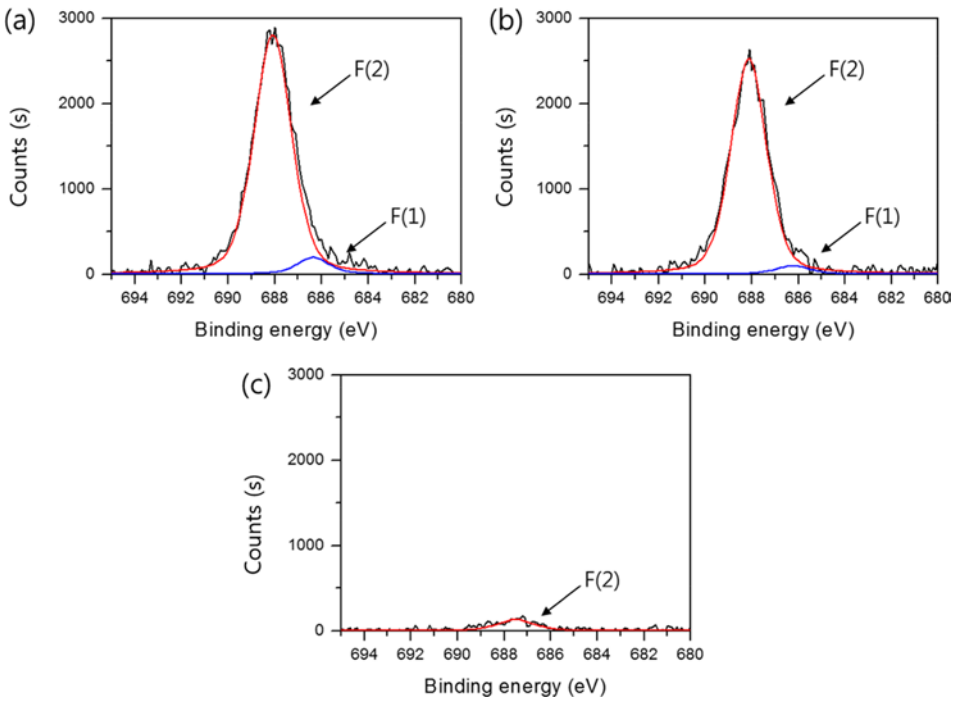

Fig. 2. Deconvolution of the core level F1s spectra of (a) G-4F, (b) G-4F-6V, and (c) G-4F-6N.

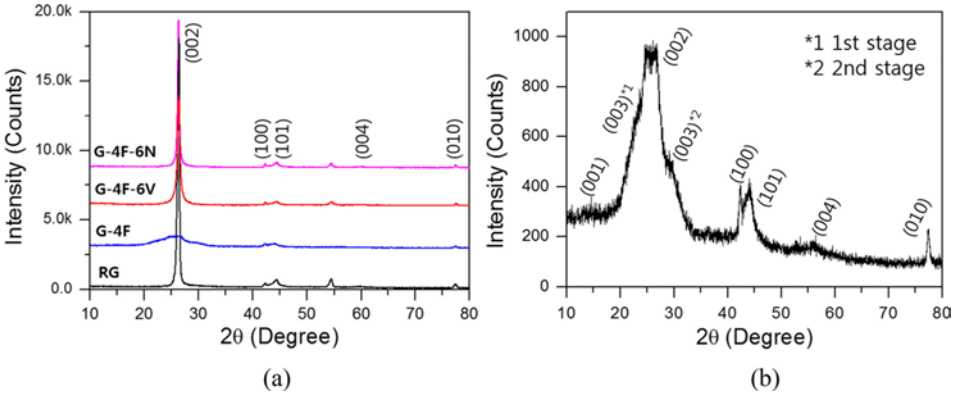

Fig. 3. XRD patterns of prepared samples (a) and G-4F (b).

decomposition gas was unstable at high temperature and under vacuum. Therefore, it is considered that unstable decomposition gases, such as F_2, re-react at high temperature on the graphite surface, in this study. Therefore, the fluorine content of G-4F-6V was almost maintained even after heat treatment.

The XRD measurements also confirm that the structures of the fluorinated graphite were drastically altered due to different heat treatment after fluorination. Fig. 3 shows the XRD diffraction patterns of prepared samples. For the RG, a strong (0 0 2) diffraction line and very weak (1 0 0), (1 0 1), (0 0 4), and (0 1 0) lines of graphite were observed [14,22]. After fluorination at 400°C, it was confirmed that the graphite structure collapsed. In Fig. 3b, fluorinated graphite at 400°C was found to contain various graphite fluoride structures, such as first-stage and second-stage structures. The (0 0 1) peak appeared to be very weak at 15°, and it was found in both the second-stage structure and graphite structure [14]. Heat treatment at 600°C of the fluorinated graphite was confirmed to return the material to a graphite structure, and the XRD results of G-4F-6V and G-4F-6N were similar to that of the graphite structure. The fluorocarbon species that evolve from fluorinated graphite are formed by the rearrangement of fluorine atoms only in the graphite galleries followed by the C–C bond cleavage of the graphite layer [21]. As the fluorocarbon species are released from the fluorinated graphite, the atoms of the graphite layer are rearranged, and the graphite structure is restored. In case of the G-4F-6V, despite changing to a graphite structure after heat treatment in a vacuum

Table 2. C1s and F1s peak parameters

Component		Peak position (eV)	Concentration (%)			
			RG	G-4F	G-4F-6N	G-4F-6V
C(1)	C–C (sp^2)	284.5	84.4	63.8	82.2	65.5
C(2)	C–C (sp^3)	285.4	8.4	8.6	12.0	8.4
C(3)	C–O	286.2	4.9	3.6	4.4	3.8
C(4)	C=O	287.1	2.4	1.8	1.5	1.8
C(5)	Semi-covalent C–F	289.1	-	22.2	-	20.5
F(1)	Ionic C–F	686.2	-	6.1	-	3.7
F(2)	Semi-covalent C–F	688.2	-	93.9	100	96.3

Table 3. Structural size parameters from X-ray diffraction

Sample	d_{002} (nm)	d_{001} (nm)	Lc_{002} (nm)	La_{101} (nm)
RG	0.337	-	20.542	19.130
G-4F	0.342	0.622	2.372	7.970
G-4F-6V	0.337	-	14.173	17.870
G-4F-6N	0.337	-	20.547	18.972

state, high fluorine content was present on the surface. Table 3 shows the structural size parameters of graphite. The d-spacing of (0 0 2) and (0 0 1), Lc_{002} and La_{101} were calculated as XRD results [23]. After fluorination at 600°C, the d_{002} increased from 0.337 nm to 0.342 nm, and d_{001} was calculated to be 0.622 nm. Further, Lc_{002} and La_{101} of G-4F were the smallest because fluorination destroys the graphite structure. As shown in Table 3, it was confirmed that the values of d_{002}, Lc, and La become similar to those of RG after heat treatment at 600°C. These results show that the graphite structure is restored after heat treatment at 600°C.

The suggested mechanism is shown in Fig. 4. It is considered that the fluorinated graphite is recovered to the graphite structure as fluorocarbon exits from the fluorinated graphite, while the unstable decomposition gas, such as F_2, re-reacts with the graphite surface during the heat treatment of the fluorinated graphite under vacuum. The F–F bond of F_2 is weak and can easily be separated by highly reactive fluorine radicals [24,25]. It is believed that the generated F_2 gas rapidly changes to a radical form, and the fluorine radical (F·) reacts rapidly with the graphite surface. Therefore, the surface fluorine concentrations of G-4F and G-4F-6V can be similar due to rapid radical reaction. Based on these results, graphite materials with high crystallinity and high fluorine content can be produced by the proposed simple and facile direct fluorination method.

Conflict of Interest

No potential conflict of interest relevant to this article was reported.

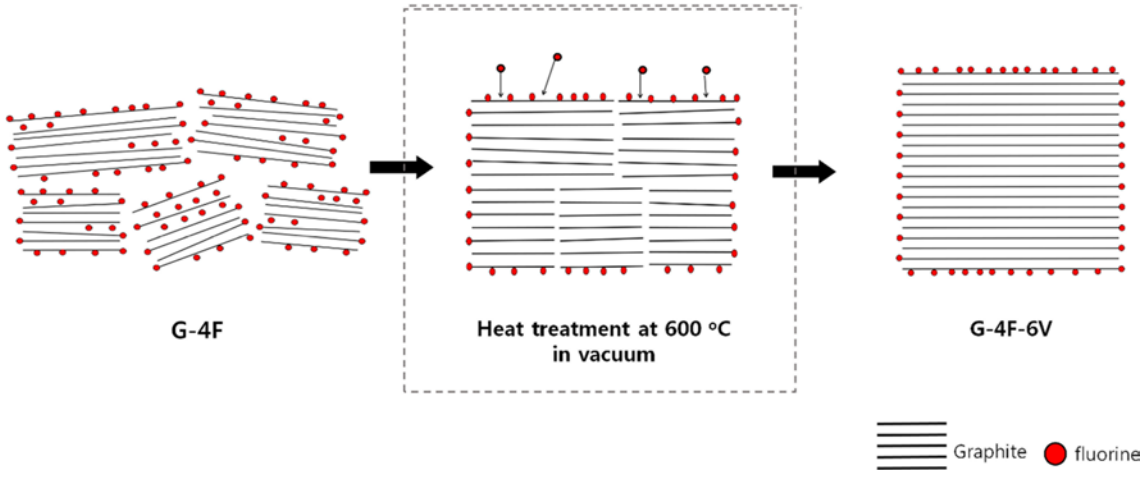

Fig. 4. Suggested mechanism of preparation of fluorinated graphite with high fluorine content and high crystallinity.

Acknowledgements

This work was supported by the Human Resources Program in Energy Technology of the Korea Institute of Energy Technology Evaluation and Planning (KETEP) granted financial resource from the Ministry of Trade, Industry & Energy, Republic of Korea (20164010201070).

References

[1] Hamwi A. Fluorine reactivity with graphite and fullerenes: fluoride derivatives and some practical electrochemical applications. J Phys Chem Solids, 57, 677 (1996). https://doi.org/10.1016/0022-3697(95)00332-0.

[2] Mar M, Ahmad Y, Guérin K, Dubois M, Batisse N. Fluorinated exfoliated graphite as cathode materials for enhanced performances in primary lithium battery. Electrochim Acta, 227, 18 (2017). https://doi.org/10.1016/j.electacta.2016.12.137.

[3] Groult H, Nakajima T, Perrigaud L, Ohzawa Y, Yashiro H, Komaba S, Kumagai N. Surface-fluorinated graphite anode materials for Li-ion batteries. J Fluorine Chem, 126, 1111 (2005). https://doi.org/10.1016/j.jfluchem.2005.03.014.

[4] Gupta V, Nakajima T, Ohzawa Y, Žemva B. A study on the formation mechanism of graphite fluorides by Raman spectroscopy. J Fluorine Chem, 120, 143 (2003). https://doi.org/10.1016/S0022-1139(02)00323-8.

[5] Kita Y, Watanabe N, Fujii Y. Chemical composition and crystal structure of graphite fluoride. J Am Chem Soc, 101, 3832 (1979). https://doi.org/10.1021/ja00508a020.

[6] Jeong E, Jung MJ, Lee SG, Kim HG, Lee YS. Role of surface fluorine in improving the electrochemical properties of Fe/MW-CNT electrodes. J Ind Eng Chem, 43, 78 (2016). https://doi.org/10.1016/j.jiec.2016.07.050.

[7] Park MS, Kim KH, Lee YS. Fluorination of single-walled carbon nanotube: the effects of fluorine on structural and electrical properties. J Ind Eng Chem, 37, 22 (2016). https://doi.org/10.1016/j.jiec.2016.03.024.

[8] Nakajima T, Gupta V, Ohzawa Y, Groult H, Mazej Z, Žemva B. Influence of cointercalated HF on the electrochemical behavior of highly fluorinated graphite. J Power Sources, 137, 80 (2004). https://doi.org/10.1016/j.jpowsour.2004.05.042.

[9] Delabarre C, Guérin K, Dubois M, Giraudet J, Fawal Z, Hamwi A. Highly fluorinated graphite prepared from graphite fluoride formed using BF_3 catalyst. J Fluorine Chem, 126, 1078 (2005). https://doi.org/10.1016/j.jfluchem.2005.03.019.

[10] Wu Z, Li J, Timmer D, Lozano K, Bose S. Study of processing variables on the electrical resistivity of conductive adhesives. Int J Adhes Adhes, 29, 488 (2009). https://doi.org/10.1016/j.ijadhadh.2008.10.003.

[11] Kabtamu DM, Chen JY, Chang UC, Wang CH. Water-activated graphite felt as a high-performance electrode for vanadium redox flow batteries. J Power Sources, 341, 270 (2017). https://doi.org/10.1016/j.jpowsour.2016.12.004.

[12] Lee KM, Lee SE, Lee YS. Improved mechanical and electromagnetic interference shielding properties of epoxy composites through the introduction of oxyfluorinated multiwalled carbon nanotubes. J Ind Eng Chem, 56, 435 (2017). https://doi.org/10.1016/j.jiec.2017.08.001.

[13] Hany P, Yazami R, Hamwi A. Low-temperature carbon fluoride for high power density lithium primary batteries. J Power Sources, 68, 708 (1997). https://doi.org/10.1016/S0378-7753(97)02642-6.

[14] Nakajima T. Fluorine-Carbon and Fluoride-Carbon Materials: Chemistry, Physics, and Applications, CRC Press, Boston (1991).

[15] Watanabe N, Shibuya A. Reaction of fluorine and carbons, and properties of their compounds. Kogyo Kagaku Zasshi, 71, 963 (1968). https://doi.org/10.1246/nikkashi1898.71.7_963.

[16] Takashima M, Watanabe N. Formation and structure of crystalline graphite fluoride. Nippon Kagaku Kaishi, 3, 432 (1975).

[17] Watanabe N, Koyama S, Imoto H. Thermal decomposition of graphite fluoride. I. Decomposition products of graphite fluoride, (CF)n in a vacuum. Bull Chem Soc Jpn, 53, 2731 (1980). https://doi.org/10.1246/bcsj.53.2731.

[18] Watanabe N, Koyama S. Thermal decomposition of graphite fluoride. II. Kinetics of thermal decomposition of (CF)n in a vacuum. Bull Chem Soc Jpn, 53, 3093 (1980). https://doi.org/10.1246/bcsj.53.3093.

[19] Watanabe N, Kawamura T, Koyama S. Thermal decomposition of graphite fluoride. III. thermal decomposition of (CF)n in oxygen atmosphere. Bull Chem Soc Jpn, 53, 3100 (1980). https://doi.org/10.1246/bcsj.53.3100.

[20] Hamwi A, Daoud M, Cousseins JC. Graphite fluoride prepared at room temperature: 1. Synthesis and characterization. Synth Met, 26, 89 (1988). https://doi.org/10.1016/0379-6779(88)90338-4.

[21] Sato Y, Hagiwara R, Ito Y. Thermal decomposition of 1st stage fluorine–graphite intercalation compounds. J Fluorine Chem, 110, 31 (2001). https://doi.org/10.1016/S0022-1139(01)00397-9.

[22] Farooq U, Doh CH, Pervez SA, Kim DH, Lee SH, Saleem M, Sim SJ, Choi JH. Rate-capability response of graphite anode materials in advanced energy storage systems: a structural comparison. Carbon Lett, 17, 39 (2016). https://doi.org/10.5714/CL.2016.17.1.039.

[23] Girgis BS, Temerk YM, Gadelrab MM, Abdullah ID. X-ray diffraction patterns of activated carbons prepared under various conditions. Carbon Lett, 8, 95 (2007). https://doi.org/10.5714/cl.2007.8.2.095.

[24] Rozen S, Brand M. Direct addition of elemental fluorine to double bonds. J Org Chem, 51, 3607 (1986). https://doi.org/10.1021/jo00369a011.

[25] Miller WT Jr, Koch SD Jr, McLafferty FW. The mechanism of fluorination. II. Free radical initiation reactions: fluorine-sensitized chlorination and oxidation. J Am Chem Soc, 78, 4992 (1956). https://doi.org/10.1021/ja01600a050.